CCC Annual Report
UIUC, August 20, 2014

Thermal Stress Cracking of Ladle Sliding Gate Plates

Hyoung-Jun Lee, Seon-Hyo Kim
Department of Materials Science & Engineering
Pohang University of Science & Technology

Brian G. Thomas
Department of Mechanical Science & Engineering
University of Illinois at Urbana-Champaign

Doo-Hoa Cheong, Sang-Woo Han, Yong-Hwan Kim
Steelmaking Research Group
POSCO Technical Research Laboratories

Research Background (Business Case)

- Longer lifetime of Sliding-Gate is needed
- JFE and POSCO are developing reusable outer plate technology
- Research is needed to understand and present cracks in ladle plates

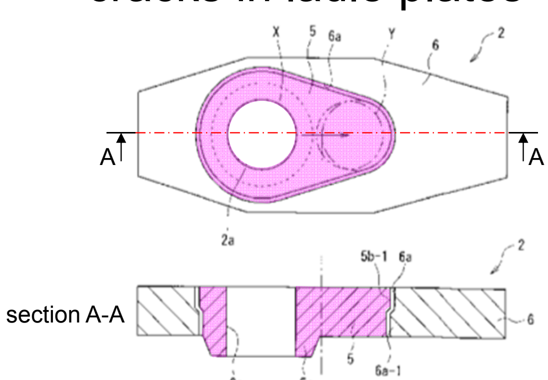

Japanese Patent [1]

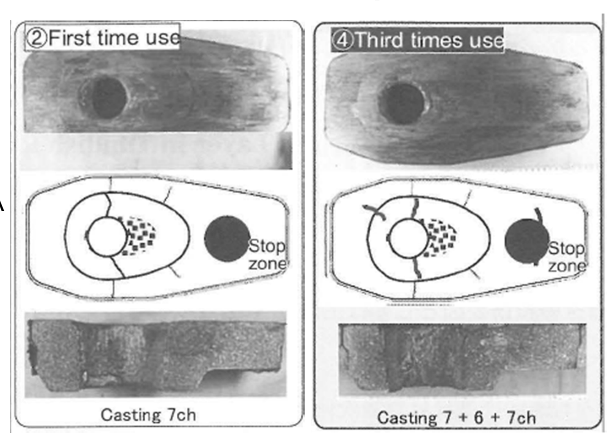

Crack location of reusable ladle plate[2]

Research Background (Operation Problems)

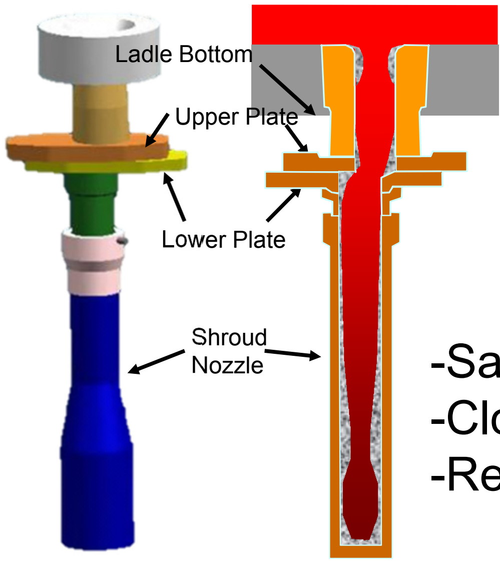

Schematic of ladle-nozzle system [3]

Why are cracks in sliding-gate a concern?

-Safety Problem (Steel leakage)
-Clogging (Air penetration)
-Require replacing plate every heat

Schematic of Ladle-Nozzle Sliding-Gate System (Animation)

Front view (opening change)

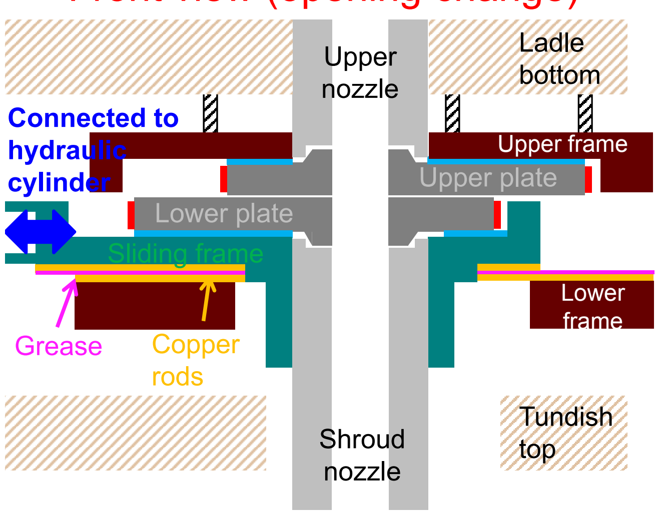

Side view (cst. pressure)

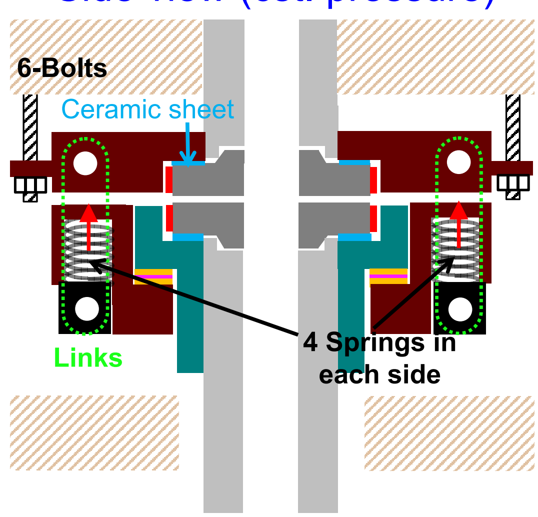

- Lower plate moves horizontally to control the molten steel flow rate through the nozzle
- Springs generate cassette pressure on the ladle plate

Type of Ladle Plate Cracks [4]

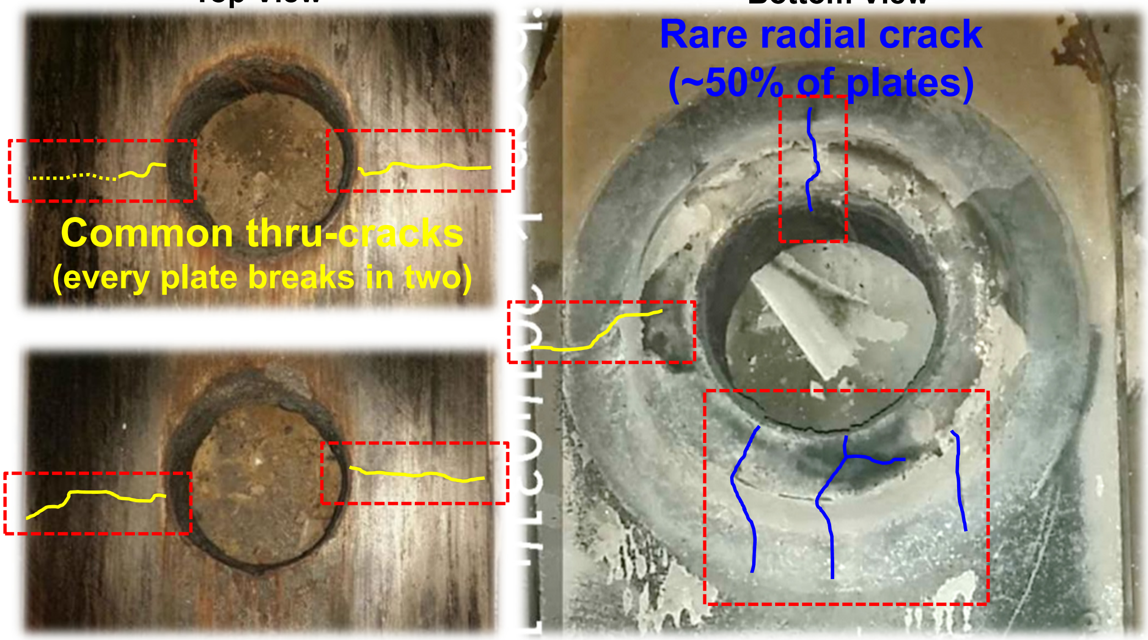

Method of Elastic Modulus Calibration by 3-Point Bending Test

Data vs time from bending test at 1200°C, #1

#	sec	kgf	mm
1	0	0	0
2	0.001	2.1	0
3	0.024	2	0.001
4	0.104	2.1	0.002
5	0.278	2.2	0.004
6	0.665	2.3	0.006
7	0.918	2.2	0.008
8	1.073	2.4	0.01
9	1.148	2.6	0.01
10	1.227	2.5	0.011
11	[illegible]	[illegible]	[illegible]
1985	168.521	[illegible]	1.404
1986	168.6	658.4	1.405
1987	168.676	658.8	1.406
1988	168.755	659.1	1.406
1989	168.833	659.6	1.407
1990	168.926	660.1	1.408
1991	169.002	660.4	1.408
1992	169.082	660.8	1.409
1993	169.157	661.1	1.41
1994	169.236	661.3	1.41
1995	169.313	661.5	1.411
1996	169.406	661.8	1.412
1997	169.483	662.1	1.412
1998	169.562	662.4	1.413
1999	169.638	662.8	1.414
2000	169.717	663.1	1.414
2001	169.794	663.4	1.445

Final load = 6505 N

Final displacement = 1.414 mm

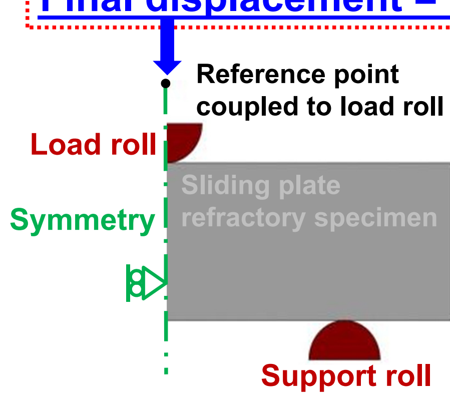

$E_{roll} = 206$ GPa

$\nu_{roll} = 0.3$

$E_{ref} = 1.53$ GPa

$\nu_{ref} = 0.2$

- Elastic modulus is adjusted until reaction force on reference point in FEM matches to final load of measurement

2-D Finite Element Model of 3-Point Bending Test

Specimen size : 20*20*80 mm
Span distance : 50 mm
Roll diameter : 10 mm

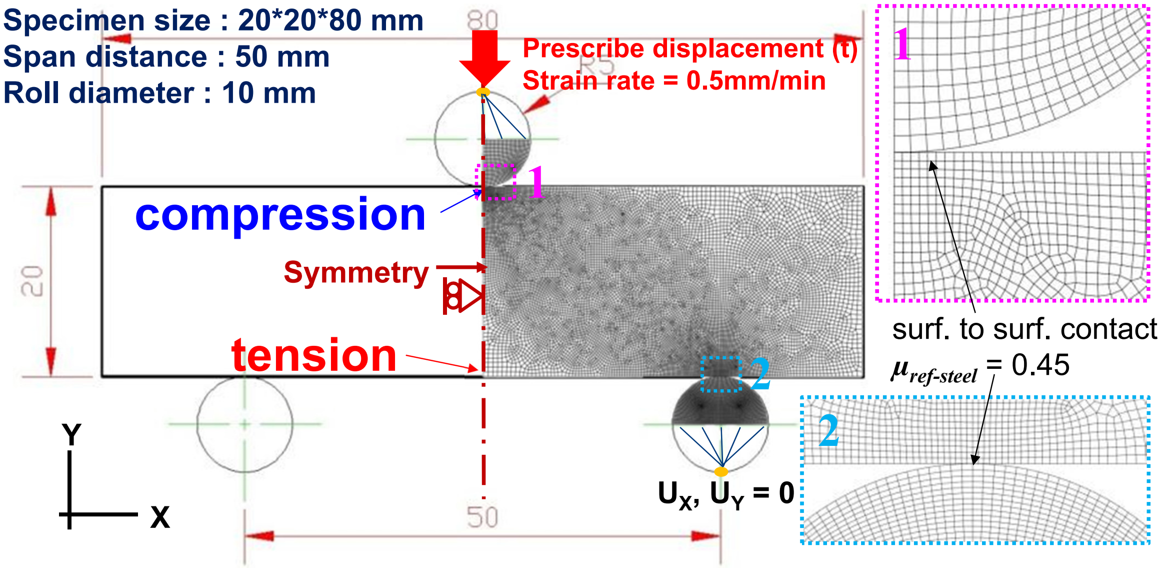

2-D transient model
Mesh : 2D plane stress
Shell thickness : 20 mm

Specimen : Hex-solid 13,093
Load roll : Hex-solid 614
Support roll : Hex-solid 3,100

3-Point Bending Test Results at Different Temperatures

Conditions		Replicated Tests			
		1	2	3	4
25 ˚C	Load(N)	2805	2266	1521	1793
	Stroke(mm)	0.160	0.117	0.116	0.155
400 ˚C	Load(N)	3474	3630	3205	-
	Stroke(mm)	0.909	0.958	0.873	-
800 ˚C	Load(N)	3366	3916	4147	-
	Stroke(mm)	0.755	1.085	1.842	-
1200 ˚C	Load(N)	6505	7234	-	-
	Stroke(mm)	1.414	1.502	-	-
1400 ˚C	Load(N)	7005	8165	-	-
	Stroke(mm)	1.598	1.925	-	-

- The lowest final load at different temperature test is input to 2-D simulation

Load vs. Displacement Measurement/Prediction

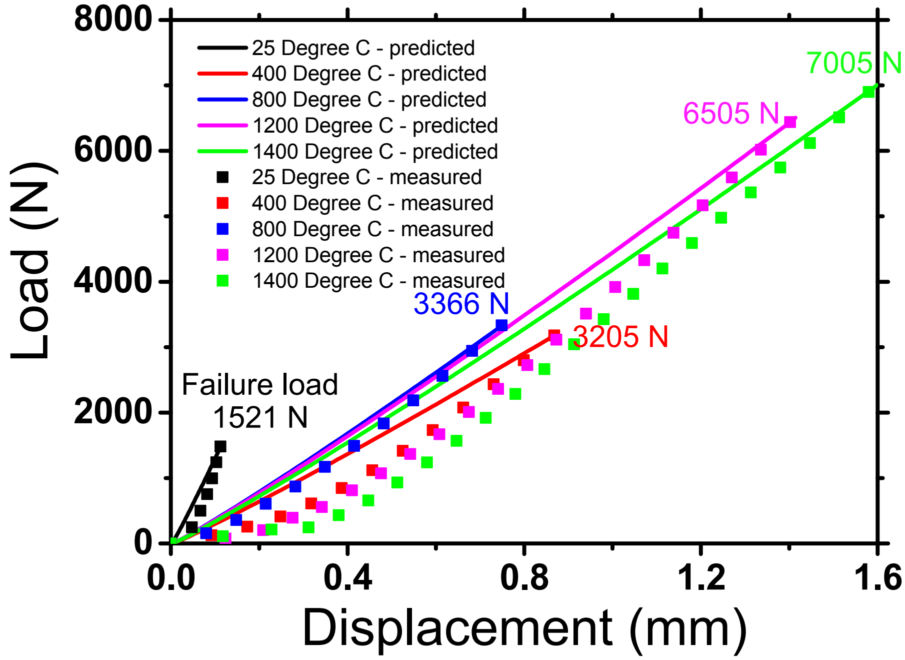

Measured and predicted final load/displacement are matched

Physical Property of Ladle Plate [5] (Chosun Refractories Co. Ltd.)

Model CSN-601N, **Alumina-Carbon Brick**			
Physical Properties		Value	
Apparent Porosity		5~8	%
Bulk Density		3,100~3,200	kg/m^3
Cold Crushing Strength		147.15 ≤	MPa
Modulus of Rupture at 1,400˚C		12.74 ≤	MPa
Thermal Expansion at 1,400˚C		0.8~1.0	%
Chemical Composition	Al_2O_3	72 ~ 76	%
	ZrO_2	4 ~ 6	%
	C	**10 ~ 13**	**%**

Analytical Solutions of 3-Point Bending Test

- Elastic modulus

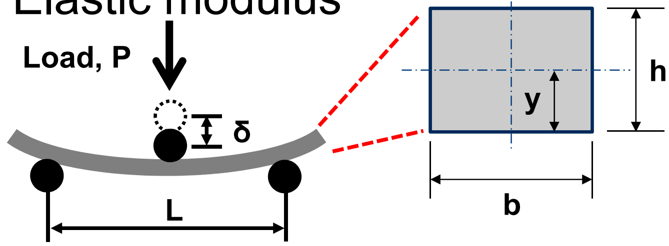

$$E_{static} = \frac{PL^3}{4bh^3\delta_{max}}$$

- Max. bending stress

$$\sigma_{max} = \frac{M}{Z} \qquad Z = \frac{I}{y} \qquad \longrightarrow \qquad \sigma_{max} = \frac{M}{I}y \qquad I = \frac{bh^3}{12}$$

$$\sigma_{max} = \frac{\frac{PL}{4}}{\frac{bh^3}{12}} \times \frac{h}{2} = \frac{3PL}{2bh^2}$$

M : Bending moment
Z : Modulus of section
I : Inertia of moment
y : Distance between centerline and top or bottom

Elastic Modulus and Critical Tensile Strength Results

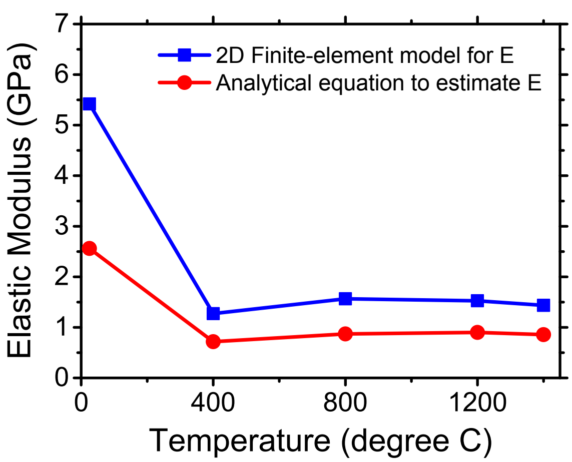

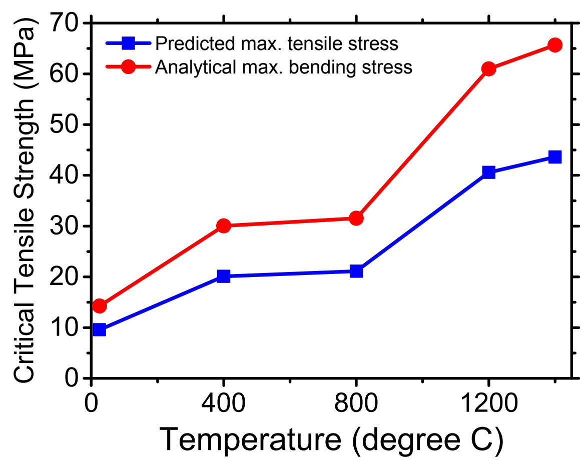

- Apparent decrease in E with increasing temperature is likely due to creep during test (when temperature exceeds glass transition temperature of ceramic)
- Predicted critical tensile strength is taken from FEM simulation at center-bottom of test piece (tension area)

Thermal Property Measurements (CSN-601N, Chosun Refractories)

Specific Heat Measurement – Ajou Univ. (Differential Scanning Calorimeter, NETZSCH, DSC200F3)

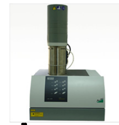

Diffusivity Measurement – KICET (Laser Flash, NETZSCH, LFA457)

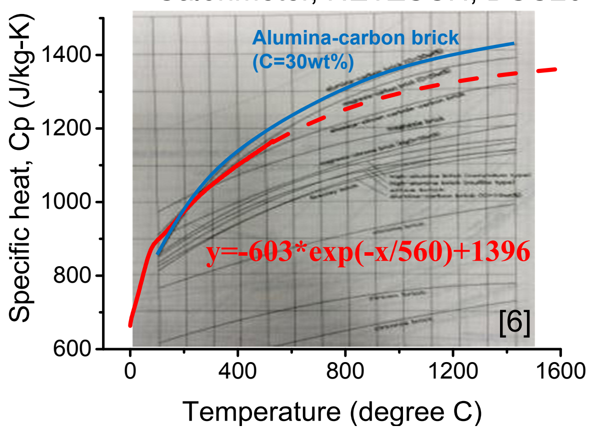

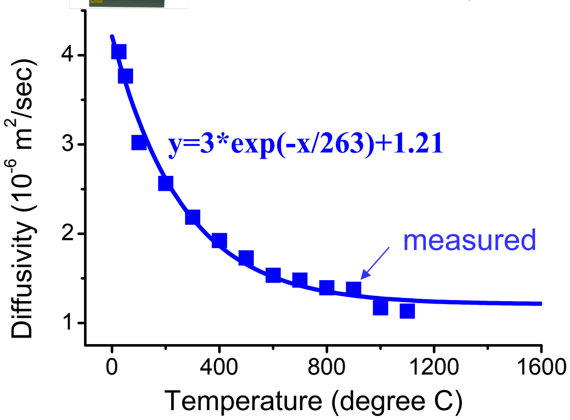

Density, measured by displacement method – POSCO = 3147.5 kg/m^3

- **Conductivity, k (W/m·K)**
  = **density, ρ (kg/m^3)** * **diffusivity, κ (m^2/sec)** * **specific heat, C_P (J/kg·K)**

Thermal Conductivity & Thermal Expansion Coefficient Evaluation

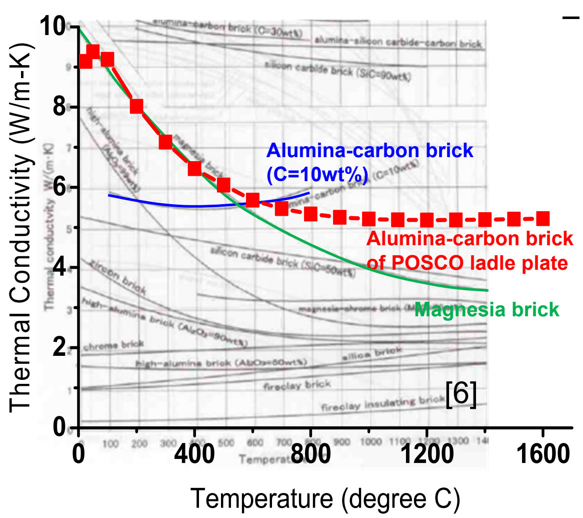

Thermal Expansion Coefficient Measurement – POSCO (Dilatometer, NETZSCH, DIL402C)

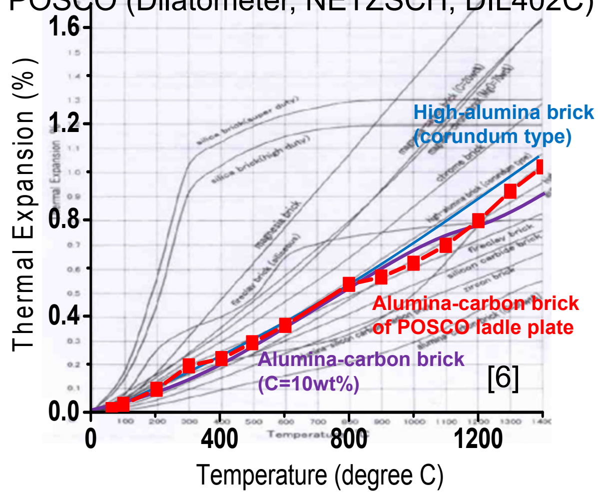

- Measured thermal properties are well matched to reference data[6]

Ladle-Nozzle Sliding-Gate Components & Cassette Pressure Calculation

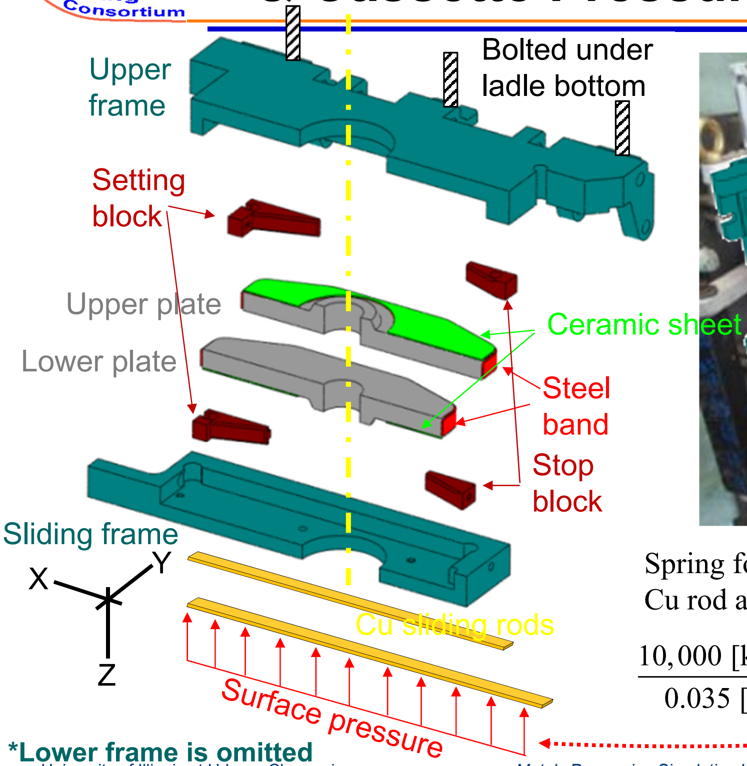

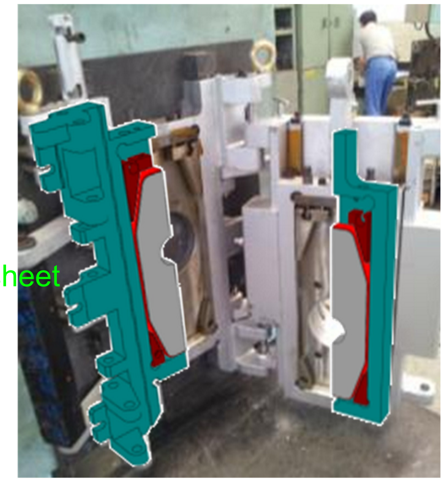

*Lower frame is omitted

Spring force = 10,000 kgf
Cu rod area = 0.035 x 0.890 m

$$\frac{10,000\ [kgf]\times 9.81\ [m/s^2]}{0.035\ [m]\times 0.890\ [m]}\times\frac{1}{2}=1.57\ [MPa]$$

Sym. model

Ladle-Nozzle Sliding-Gate Domain / Finite Element Mesh

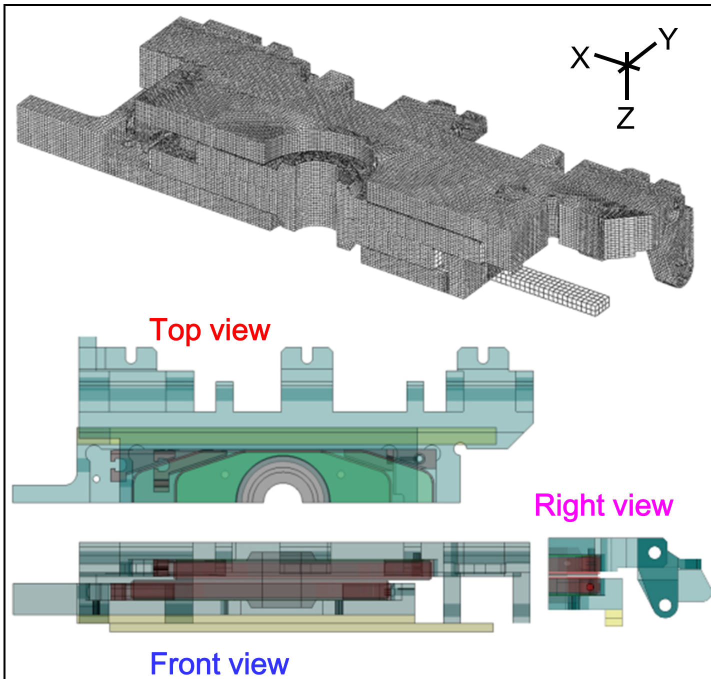

Parts	Elements	
	Hexahedral	Wedge
Upper plate	-	47,764
Upper band	288	-
Upper ceramic sheet	-	901
Upper stop block	3,226	-
Upper setting block	2,520	-
Upper frame	147,983	-
Lower plate	-	47,764
Lower band	288	-
Lower ceramic sheet	-	901
Lower stop block	-	2,495
Lower setting block	1,793	-
Sliding frame	51,328	-
Sliding frame Cu rod	632	
Lower frame Cu rod	720	
Total elements	308,603	

Calculation time : 1.5 hrs. (heat transfer), 30 hrs. (stress)

Properties for Ladle-Nozzle Sliding-Gate Model

	Property		Value	
Refractory (Plate)	Density	ρ_{ref}	3147.5	kg/m^3
	Elastic modulus	E_{ref}	Prescribed	Pa
	Poisson's ratio	ν_{ref}	0.2	-
	Thermal conductivity	k_{ref}	Prescribed	W/m·K
	Specific heat	$C_{p,ref}$	Prescribed	J/kg·°C
	Expansion coefficient	α_{ref}	Prescribed	$°C^{-1}$
	Emissivity [7]	ε_{ref}	0.92	-
Steel (Band, Cassette) [7]	Density	ρ_{steel}	7860	kg/m^3
	Elastic modulus	E_{steel}	206×10^9	Pa
	Poisson's ratio	ν_{steel}	0.3	-
	Thermal conductivity	k_{steel}	48.6	W/m·K
	Specific heat	$C_{p,steel}$	418.6	J/kg·°C
	Expansion coefficient	α_{steel}	1.78×10^{-5}	$°C^{-1}$
	Emissivity	ε_{steel}	0.75	-
Friction coefficient	Steel-Steel [8]	$\mu_{steel\text{-}steel}$	0.3	-
	Steel-Refractory [7]	$\mu_{steel\text{-}ref}$	0.45	-
	Refractory-Refractory [7]	$\mu_{ref\text{-}ref}$	0.1	-
	Stefan-Boltzmann constant	σ	5.669×10^{-8}	$W/m^2 \cdot K^4$

Variables and Boundary Conditions for Ladle Sliding-Gate Model

Surface pressure 10,000 kgf at Cu sliding rod

Lower plate movement with 25 mm/min.

			Preheating	Refining	Casting	
Opening Ratio [4]		-	100	0	70	%
Duration Time [4]		t	210	160	33	min.
Initial Temperature		$T_{initial}$	25	-	-	°C
Internal Sink Temperature		T_i	750 [9] (Gas)	340 [10] (Ladle filler)	1600 (Molten Steel)	°C
Internal Convection Heat Transfer Coefficient (Forced) [9]		h_i	65.24	8.82	28.7×10^3	$W/m^2 \cdot K$
External Ambient Temperature [9]	Inside of Cassette area	$T_{o,in}$	200	200	270	°C
	Outside of Cassette area	$T_{o,out}$	100	100	120	°C
External Convection Heat Transfer Coefficient (Free) [9]		h_o	8.82	8.82	8.82	$W/m^2 \cdot K$

Thermal Behavior (Movie)

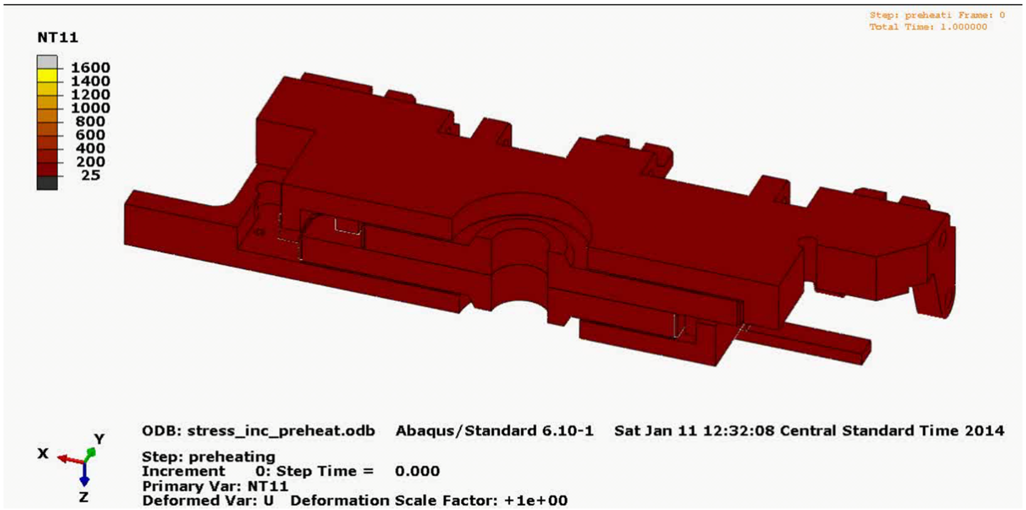

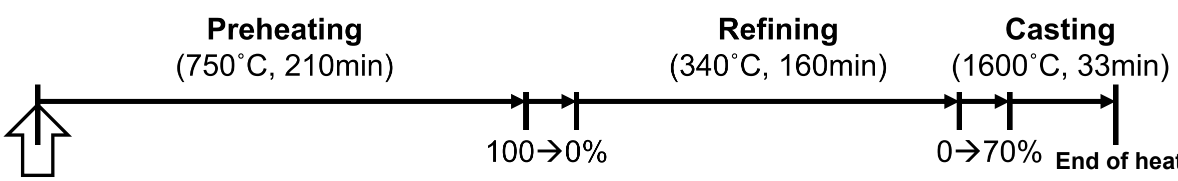

Temperature & Hoop Stress Histories at Locations where Cracks are Observed

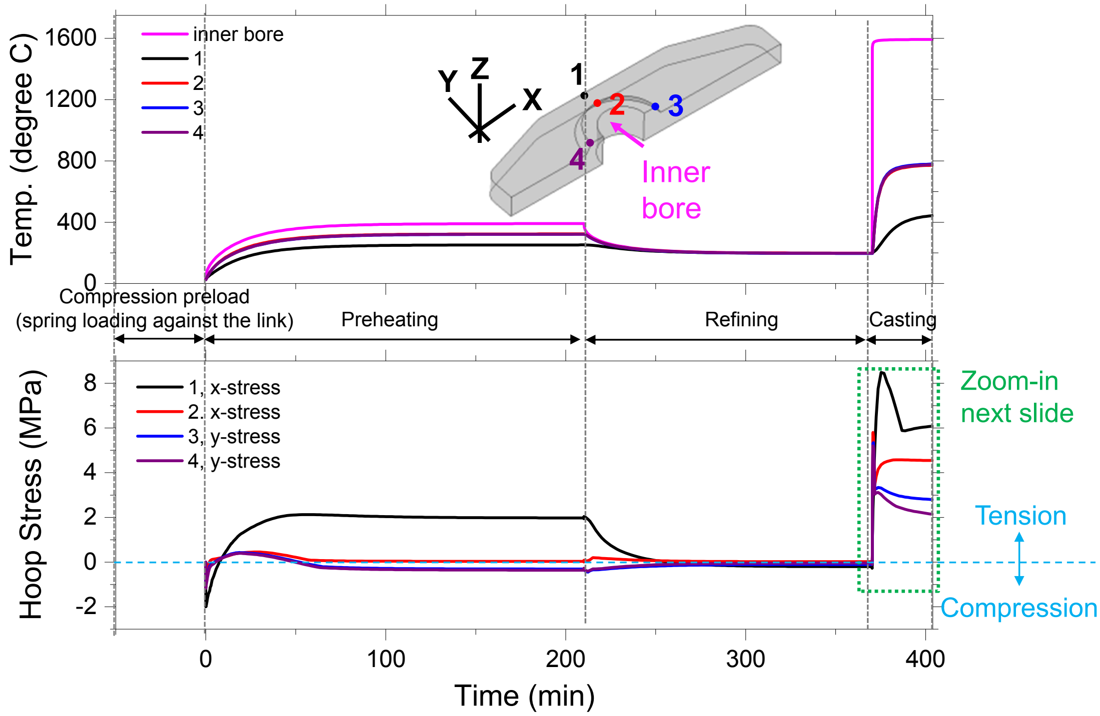

Temperature & Hoop Stress Histories during Casting (Log Scale on x-axis)

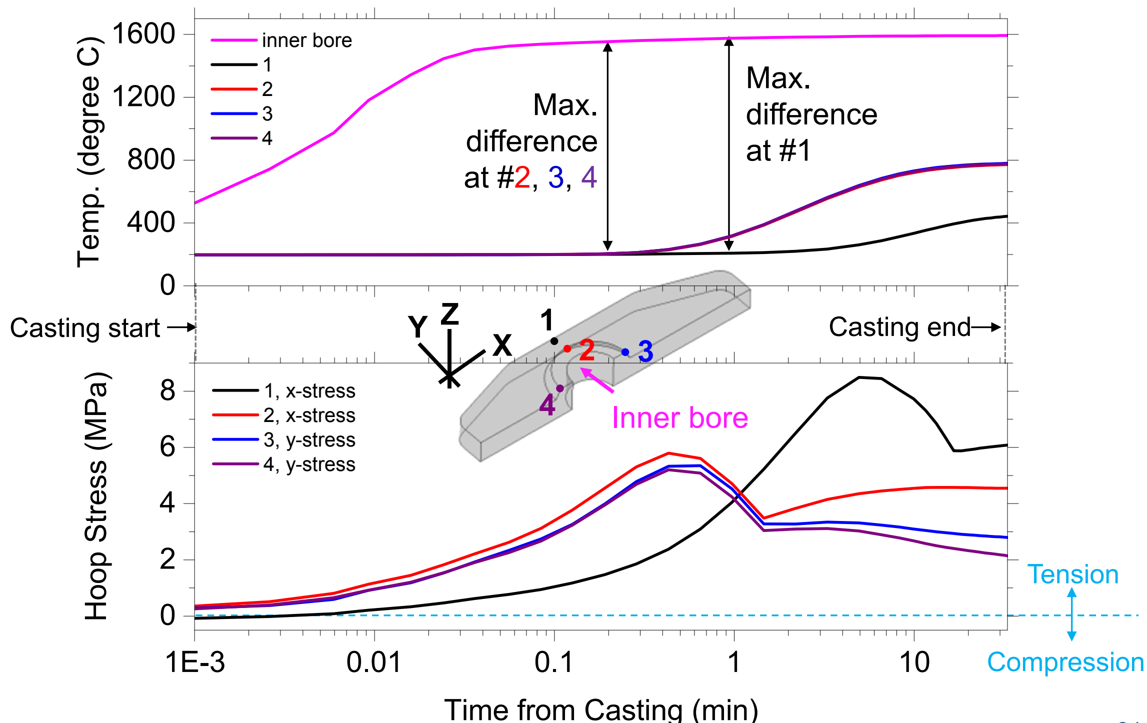

Common Through-thickness Crack Formation Mechanism

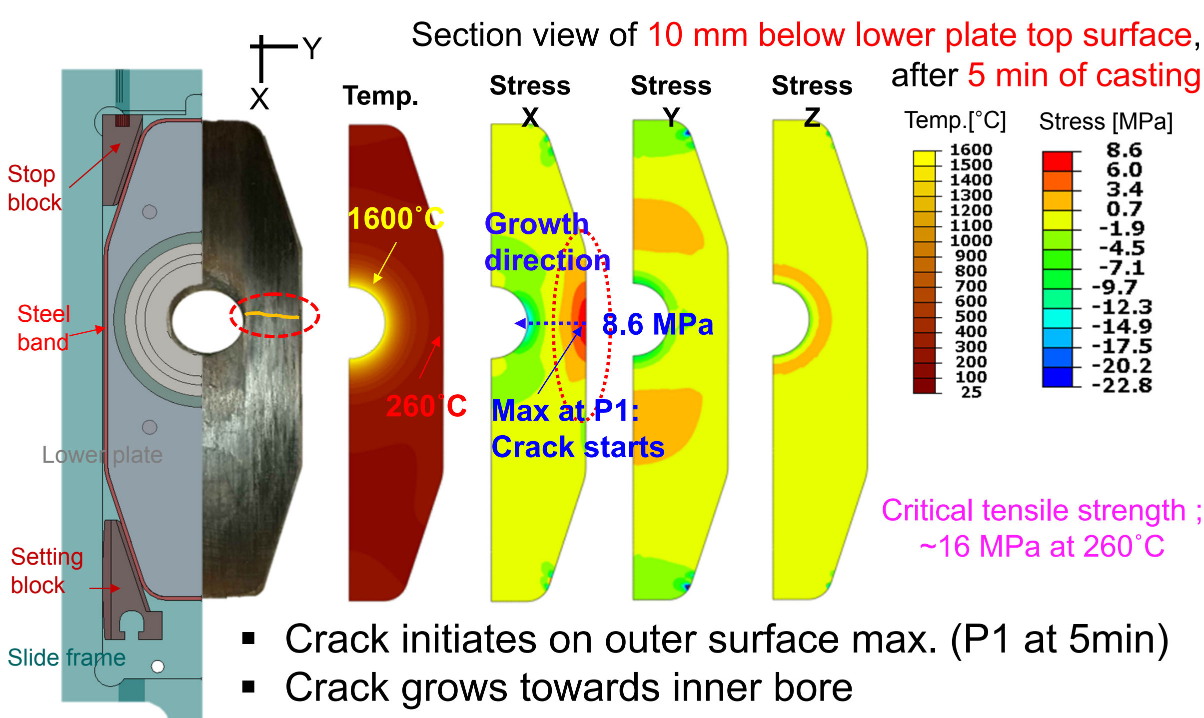

- Crack initiates on outer surface max. (P1 at 5min)
- Crack grows towards inner bore

Rare Radial Crack Formation Mechanism

View of lower plate, after 0.5 min of casting

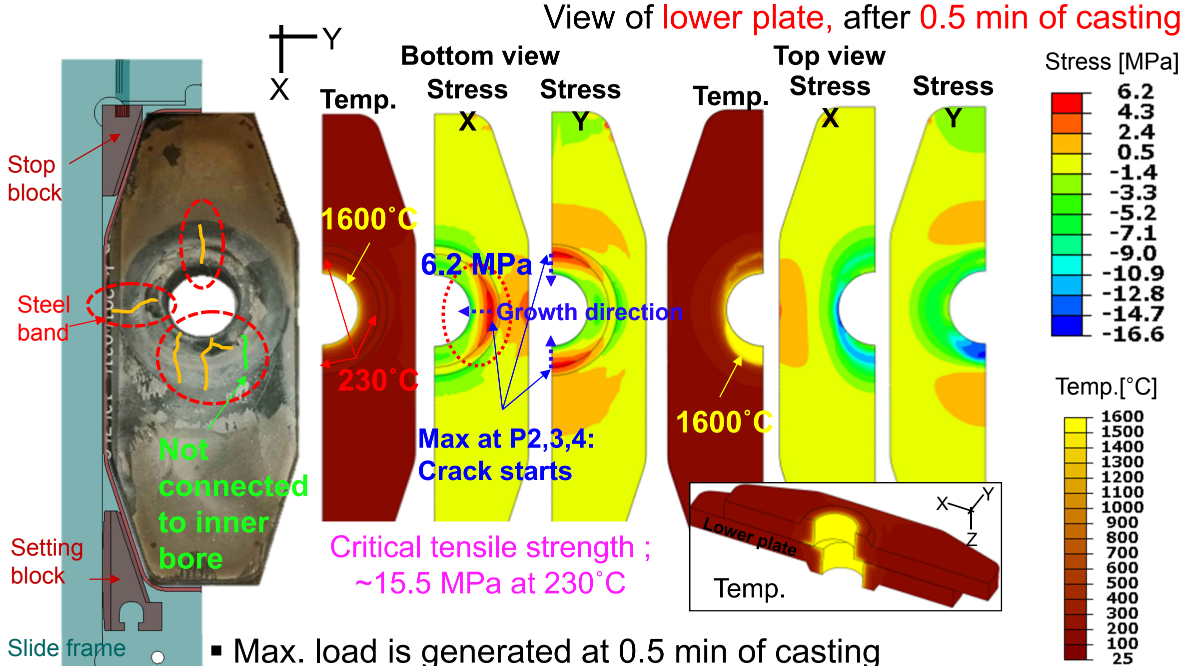

- Max. load is generated at 0.5 min of casting
- Crack starts on convex (colder) lump part of upper or lower plate

Mechanical Loading Effects

Temp. and stress distribution in plates at the end of casting

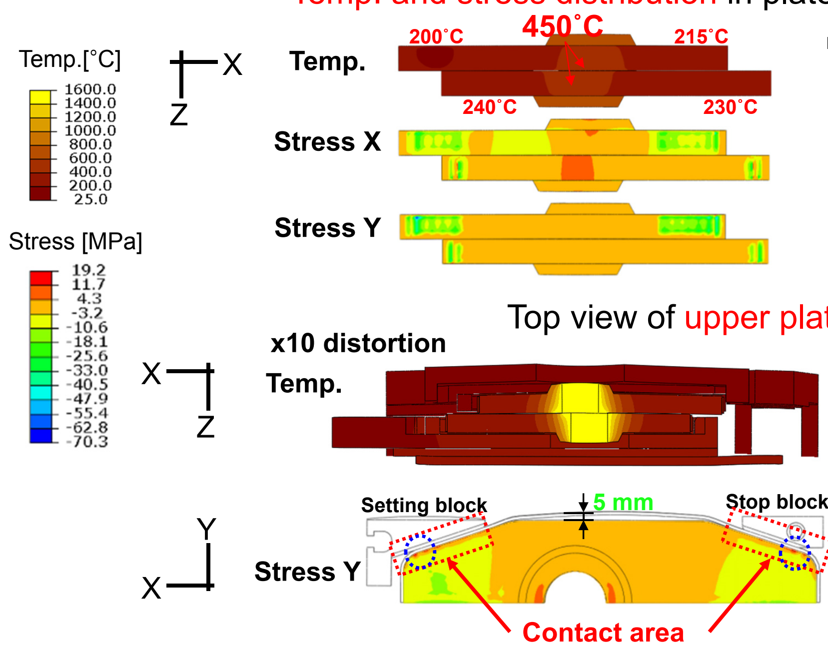

- Highest temperature causes compression against block
- Misalignment during assembly leads to concentrated point loads at contact points

Note: steel band expands away from ceramic, leaving ~5mm gap during casting

Casting Result without Preheating (Worst Case)

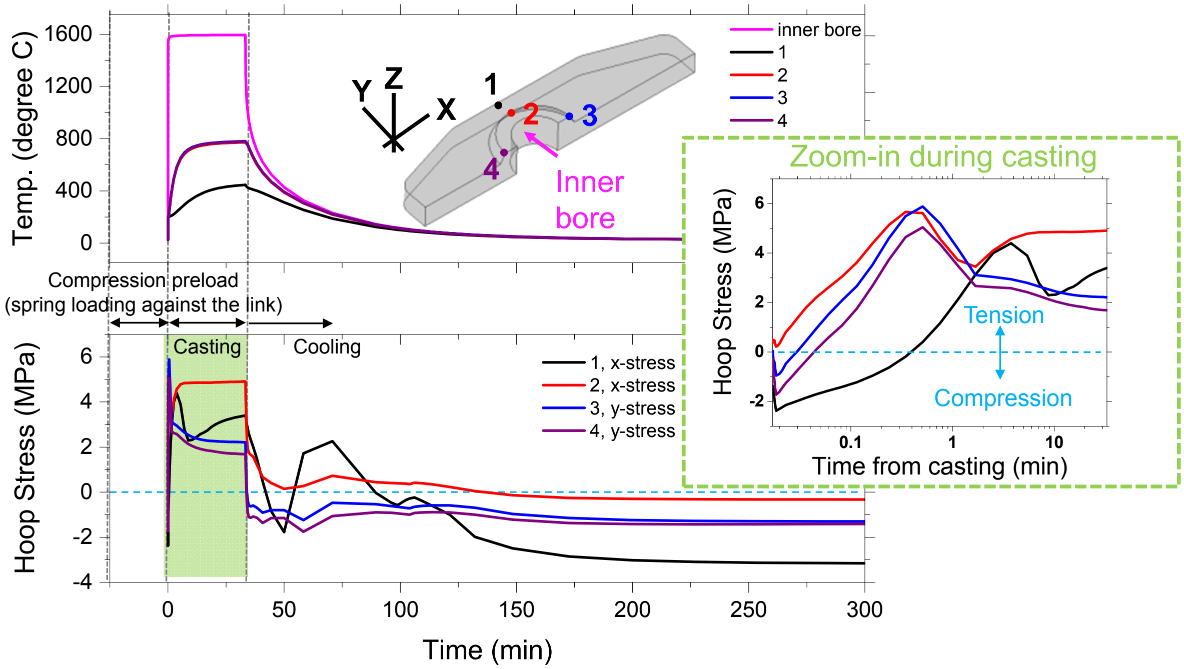

Direct casting and cooling is simulated without preheating for worst case

Thermal/Mechanical Distortion Affected by Cassette Pressure

Stress histories, x 10 distortion

Front view - symmetric plane, XZ (Stress X)

Right mirror view (Stress Y)

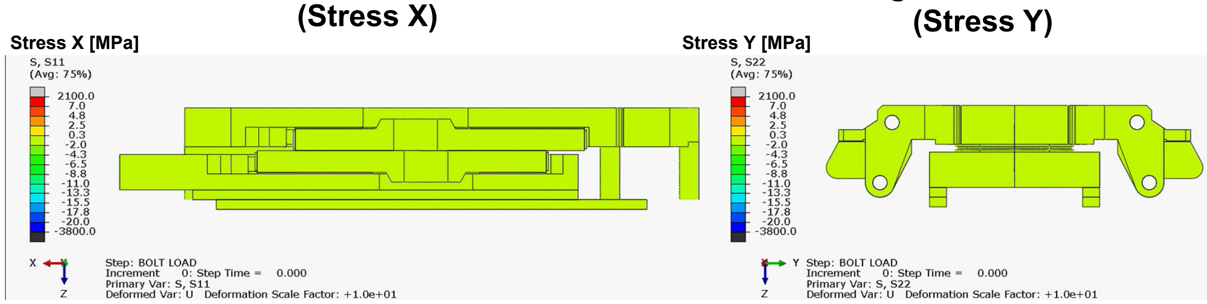

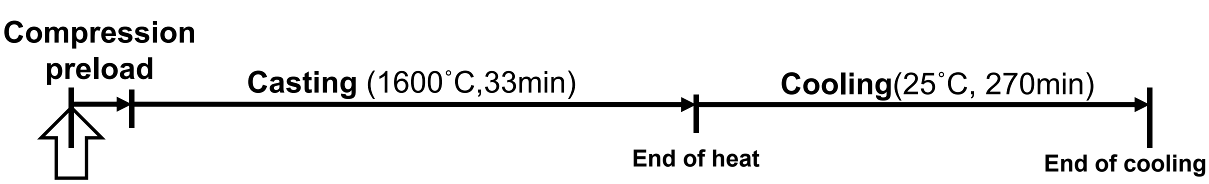

Cassette is plastically deformed after several times using for casting according to plant engineer – Deformation shape effects of plate in the plant will be discussed in future work

Future Works

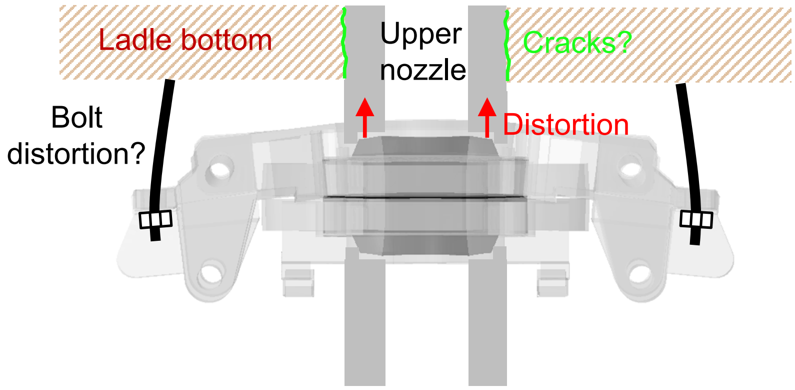

- **Plastic deformation of used cassette in the plant is needed to investigate**
  - Thermal and mechanical distortion of ladle-nozzle system pushes against upper nozzle, creating forces between upper nozzle and ladle bottom refractory
- **Creep effect in ceramic materials is important for cracking**

Reusable Ladle-Nozzle Sliding-Gate Domain / Finite Element Mesh

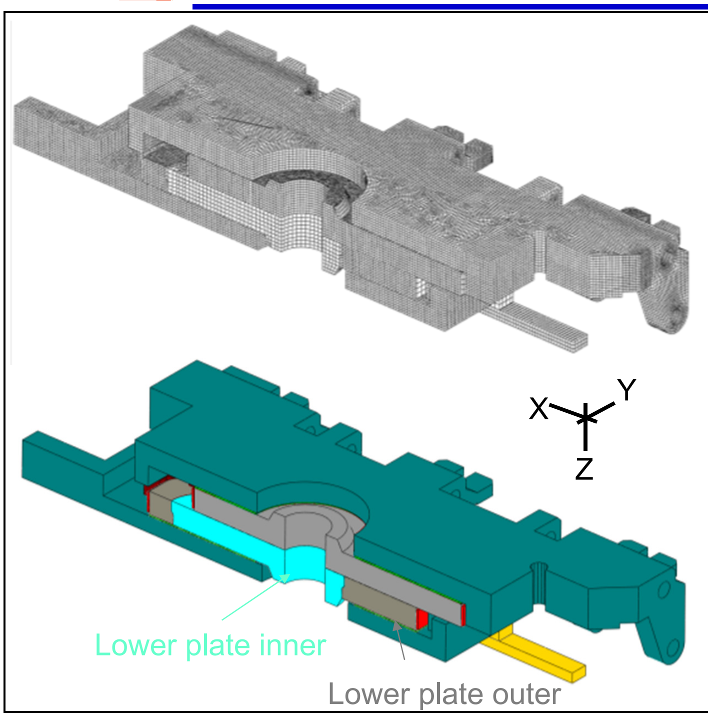

Part		Elements	
		Hexahedral	Wedge
Upper plate		-	49,452
Upper band		288	-
Upper Ceramic sheet		-	897
Upper stop block		1,729	-
Upper setting block		2,749	-
Upper frame		146,671	-
Lower Plate	Inner	-	5,673
	Outer	-	31,150
Lower band		288	-
Lower ceramic sheet		-	897
Lower stop block		-	1,729
Lower setting block		2,749	-
Sliding frame		59,164	-
Sliding frame Cu rod		632	
Lower frame Cu rod		2,664	
Total elements		306,732	

Reusable Lower Plate
Domain / Finite Element Mesh

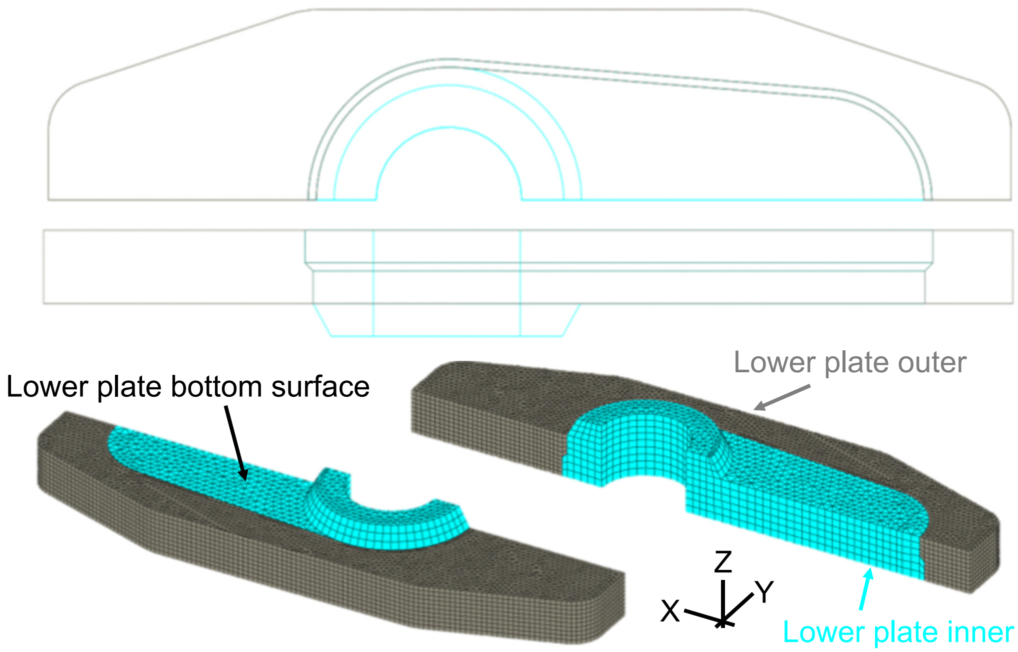

Hoop Stress Results Comparison
(Conventional / Reusable)

Section view of 10 mm below lower plate top surface, after 5 min of casting

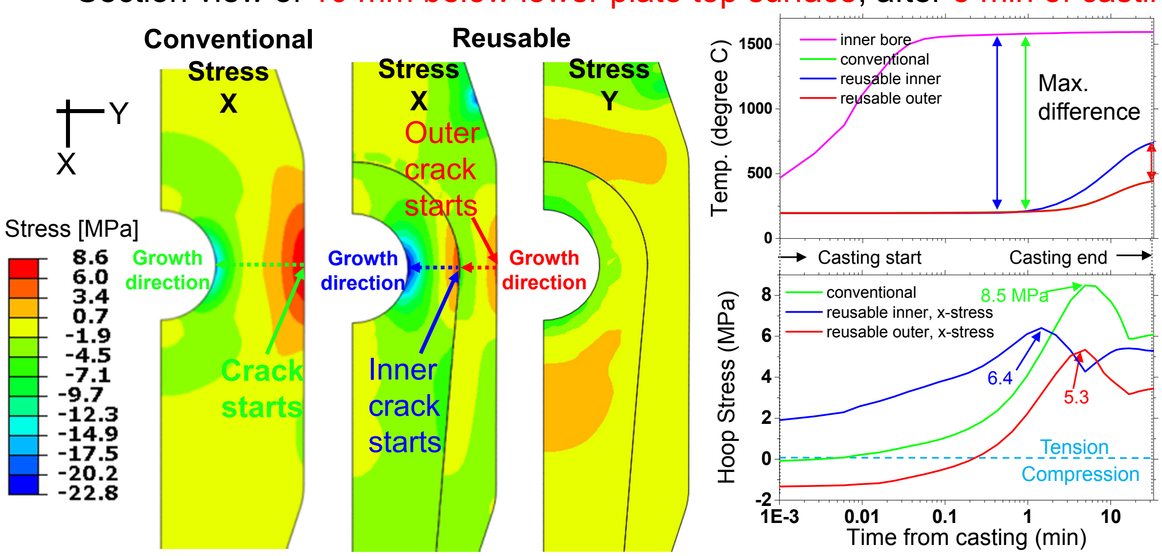

- Larger temperature difference between inside and outside surfaces generates larger tensile stress
- Tensile stress can be reduced by using outer “reusable” plate

Reusable Lower Plate Outer Crack Formation Mechanism

Top view of reusable lower plate top surface, after 5 min of casting

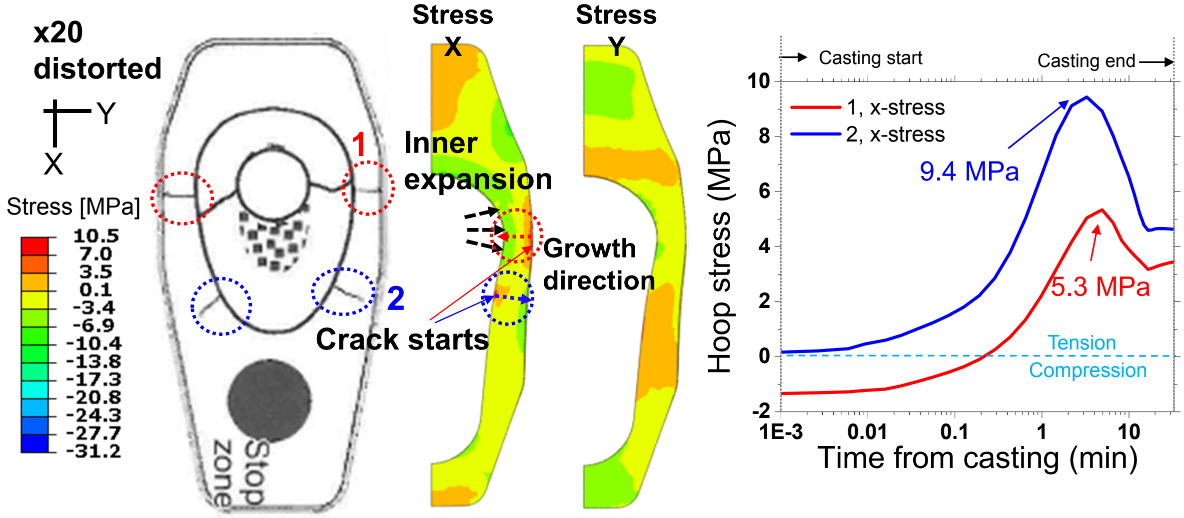

Crack locations after once use [2]

- Crack locations are well matched to used plate
- In addition to same common crack mechanism:
  Expansion of inner plate causes tension in reusable outer plate

Conclusions

- Replicated 3-point bending tests measured refractory strengths at different temps.
- Thermal expansion of hot inside of plate causes exterior tensile hoop stress and crack growth towards interior: leading to both common through thickness cracks (starting at cold outside of plate) and rare radial cracks (starting at cold outside of lump).
- No cracks are predicted (so quantitative models and fracture criteria need more work.
- Reusable plate are predicted to reduce tensile hoop stress, but through-thickness crack formation may be unavoidable.
- Two different crack mechanisms can form through-thickness cracks in reusable outer plate middle.

Acknowledgments

- Continuous Casting Consortium Members (ABB, ArcelorMittal, Baosteel, Magnesita Refractories, Nippon Steel and Sumitomo Metal Corp., Nucor Steel, Postech/ Posco, Severstal, SSAB, Tata Steel, ANSYS/ Fluent)
- Others
  - Chosun Refractories Co. Ltd.
  - Daejoo Machinery Co. Ltd.
  - POSCO Grant # 4.0009576.01

References

[1] Japanese Patent, JP2012-121049A, 2012.6.28

[2] T. Hisanaga, et al., Japanese Journal of Refractories, No.1, pp.26, 2012

[3] J. Choi, POSCO Gwangyang works, Gwangyang, Jeonnam, Korea

[4] D.H. Jeong, et al.. POSCO Technical Research Lab., Pohang, Gyeungbuk, Korea, 2013

[5] Technical Data, Chosun Refractories Co. Ltd., http://www.chosunref.co.kr/home/kor/product/ndata/

[6] T.G. Kyokai, Refractories Handbook, The Technical Association of Refractories, Japan, June, 1998

[7] J.M. Sun, et al., Chosun Refractories Co. Ltd. Research Center, Pohang, Gyeongbuk, Korea, 2010

[8] B.G. Thomas, et al., Iron and steel maker, Vol.25, pp.125, 1998

[9] H.J. Lee, et al., “Thermal Stress Cracking of Sliding Gate Plates”, AISTech proceeding, 2012

[10] S.S. Kim, et al., Journal of Ceramic Society, Vol.38, No.9, pp.829, 2001